Journal of Energy

VOLUME 67 Number 3 | 2018 Special Issue

journal homepage: http://journalofenergy.com/

D. GORENC
K. FLEGAR
I. LONČAR

KONČAR – Apparatus and Switchgear
CROATIA

E. PLAVEC

KONČAR – Electrical Engineering Institute
CROATIA

Simulation and Measurement of Pressure Rise in GIS 145 kV due to Internal Arcing

SUMMARY

Internal arc testing of metal-enclosed, SF_6 gas insulated switchgear (GIS) is defined by IEC 62271-203 and is not a part of mandatory type tests. However, due to the increasing demands on the safety of personnel, more often the implementation of this test is required in the tender documentation. According to IEC, the duration of the electric arc is related to the performance of the protective system determined by the first and second stage of protection. For the rated short-circuit current equal or higher than 40 kA, during the first stage of protection (0.1 s), no external effects on enclosure other than the operation of pressure relief device is permitted. During the second stage of protection (≤0.3 s) no fragmentation is permitted, but burn-through is acceptable. The test should be carried out on the GIS compartment with the smallest volume at nominal gas pressure. Since a newly developed GIS 145 kV is designed as a three-phase encapsulated, arc initiation is achieved by short connecting of all three phase conductors in the vicinity of a partition by means of a thin metal wire. This ensures that two electric arcs burn simultaneously commutating between the phases, so the possibility of enclosure burn-through in this type of GIS is minimized. In order to prevent the release of SF_6 gas in the atmosphere during the testing, a test enclosure should be placed in a protective gastight enclosure filled with air or more often SF_6 gas at pressure of 0.1 MPa. This test object configuration significantly complicates the pressure rise calculation and increases the testing cost. In order to prevent enclosure fragmentation, the pressure difference between the test enclosure and the protective enclosure during the test should always be less than the bursting pressure of test enclosure. Also, the protective enclosure should be designed to withstand the maximum pressure rise that may occur after pressure relief device opens. In order to assess the likelihood of passing the upcoming type test for newly developed GIS, a computer program for calculation of pressure and temperature in the test enclosure and protective enclosure was developed. The mathematical model is based on the paper of the working group CIGRE A3.24, published in 2014. The basic model shown in the paper is enhanced by the real properties of the SF_6 gas/plasma, evaporation of the electrode material and the insulator ablation. The contribution of exothermic/endothermic reactions between the gas and the electrode material on the pressure and temperature rise was also considered. At the same time, the measurements of pressure rise in GIS enclosure and protective enclosure were carried out in Končar High Power Laboratory. The experiments performed on a copper and aluminum electrodes in SF_6 gas confirmed significantly higher contribution of aluminum electrodes to the pressure and temperature rise compared to the copper electrodes. The computer program is verified by measurement results.

KEYWORDS

GIS, internal arc test, protective enclosure, pressure rise, test enclosure

INTRODUCTION

Internal arc testing of metal-enclosed, gas insulated switchgear (GIS) 145 kV is defined by IEC standard [1] and is not a part of mandatory type tests. However, due to the increasing demands on the safety of personnel, more often the implementation of this test is required in the tender documentation. According to IEC, the duration of the electric arc is related to the performance of the protective system determined by the first stage (main) and second stage (back-up) protection. For the rated short circuit current equal or greater than 40 kA, the recommended current duration is 0.1 s for the first protection stage and less than or equal to 0.3 s for the second protection stage (Table I). The criteria for a successful test are that there is no external effect other than the operation of pressure relief devices in the first 0.1 s of current duration and that there is no fragmentation of enclosure after 0.3 s of current duration, burn-through is acceptable.

Table I Recommended arc duration and the criteria for passing the test according to [1]

Rated short-circuit current	Protection stage	Duration of current	Performance criteria
<40 kA r.m.s.	1	0.2 s	No external effect other than the operation of suitable pressure relief devices
	2	≤0.5 s	No fragmentation (burn-through is acceptable)
³40 kA r.m.s.	1	0.1 s	No external effect other than the operation of suitable pressure relief devices
	2	≤0.3 s	No fragmentation (burn-through is acceptable)

D. Gorenc, K. Flegar, I. Lončar, E. Plavec, Simulation and Measurement of Pressure Rise in GIS 145 kV due to Internal Arcing, Journal of Energy, vol. 67 Number 3 (2018), Special Issue, p. 14–19

The compartment of GIS which appear to have the least likelihood of withstanding the pressure and temperature rise in the event of arcing shall be selected for test. In practice, this means the compartment with the smallest volume. The testing is performed at nominal SF_6 gas pressure in the test enclosure. The specified standard allows the test results obtained in a single compartment to be used in calculating and proving the resistance of other gas compartments on internal arc.

PHYSICAL PROCESSES IN GIS COMPARTMENT DUE TO INTERNAL ARC

When the arc burns between the phase conductors, evaporation of the electrode material occur. The specific energy of evaporation for various electrode materials are given in Table II [2], they include the energy required for heating to the melting temperature, melting, heating to the evaporation temperature and evaporation. The evaporated electrode material is mixed with SF_6 gas in arc compartment and the chemical reactions occur. In the exothermic chemical reaction between evaporated aluminum and SF_6 gas (or oxygen) more heat is generated than it is required for evaporation of the same amount of aluminum (Table II). On the other hand, in the reaction between the evaporated copper and the oxygen, less heat is developed than it is required for copper evaporation, because of that the reaction is endothermic. The data for the reaction between evaporated copper and SF_6 gas were not found in the references.

If the arc burns in the vicinity of bushing plate, ablation or evaporation of the insulation material occurs. The bushing plates are mainly made of epoxy resin and glass-based fillers. It is assumed that methane gas (CH_4) is the only gaseous product of bushing plate ablation [3]. If the gas temperature in the arc compartment is sufficiently high, gas degradation occurs and at the highest temperatures plasma formation occurs. Between the products of gas degradation and evaporated electrode material chemical reactions and formation of new products occur. This also leads to the change in thermodynamic properties of gas/plasma. Assuming the local thermodynamic equilibrium (all gas/plasma particles are at the same temperature), thermodynamic properties of gas/plasma are the functions of temperature, pressure and mass concentration of individual reactants.

Table II Specific energy of evaporation, chemical reactions and generated specific heat for various electrode materials and surrounding gas

Electrode material	Specific energy of evaporation [MJ/kg]	Molar mass [g/mol]	Exothermic/endothermic reactions	Specific generated heat [MJ/kg]
Al	13.73	26.98	$Al+\frac{3}{2}SF_6 \rightarrow AlF_3+\frac{3}{2}SF_4+850\ kJ$	31.5
			$Al+\frac{3}{4}O_2 \rightarrow \frac{1}{2}Al_2O_3+837\ kJ$	31
Cu	6.18	63.54	$Cu+\frac{1}{4}O_2 \rightarrow \frac{1}{2}Cu_2O+75\ kJ$	1.2
Fe	8.04	55.85	$Fe+\frac{1}{2}O_2 \rightarrow FeO+250\ kJ$	4.5

MATHEMATICAL MODEL

The basic layout for calculation of pressure and temperature rise in GIS enclosure and protective enclosure is shown in Fig. 1 [3]. The GIS test compartment is represented by arc compartment, and the protective enclosure with exhaust compartment. Between the arc and exhaust compartment there is a bursting disc which opens at predefined pressure. Although there can also exist bursting disc between the exhaust compartment and installation room/environment, its function is solely for safety, i.e. under normal conditions during the testing no opening is expected.

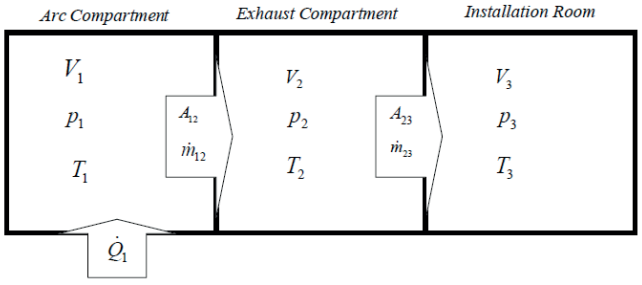

Fig. 1 Basic layout and variables used in calculation [3]

Several computer programs have been made for calculation of pressure and temperature rise due to internal arcing inside the test compartment and protective enclosure. Mathematical models are based on the report of the working group A3.24 CIGRE [3]. This paper presents two models: the basic model with constant properties of gas already shown in [3] and enhanced model with real gas/plasma properties which considers evaporation of electrodes material, ablation of an insulators and the contribution of exothermic/endothermic reactions to pressure and temperature rise. Both models assume the uniformly distribution of temperature, pressure and other gas parameters in the arc compartment and exhaust compartment, respectively. Along with known initial conditions, the Euler's method was used to integrate ordinary differential equations. The total phenomenon duration is divided into a series of short intervals Δt in which calculation of temperature and mass change of gas are performed, and at the end of each interval the new values of temperature, pressure and mass of gas in the enclosures are calculated. The described computer program was made in Matlab.

The basic model with constant gas properties

The equations for pressure and temperature rise in arc and exhaust compartments are based on the assumption of ideal gas, meaning that the thermodynamic properties of gas, C_p, C_v, R_s and k, are constant and taken at gas temperature of 300 K and a pressure of 0.1 MPa (Table III). Since in reality the thermodynamic properties of gas/plasma change with the temperature, pressure and mass concentration of individual reactants, this model is applicable for SF_6 gas temperature up to 2000 K and air temperature up to 6000 K. The model does not consider the evaporation of electrode material neither the ablation of an insulation material. The contribution of exothermic/endothermic reaction to the temperature and pressure rise is considered by "artificial" increase of k_p factor, which shows how much electrical energy is consumed to heat the gas. According to [3], for copper electrodes, the value of k_p factor is between 0.5 and 0.7, while the value for aluminum electrodes can be significantly higher than 1 (up to 1.6).

Table III Thermodynamic properties of air and SF6 gas at T=300 K and p=0.1 MPa [3]

Thermodynamic properties of gas	Label	Air	SF_6	Measurement unit
Specific heat capacity at constant volume	C_v	716	608	J/(kgK)
Specific heat capacity at constant pressure	C_p	1005	665	J/(kgK)
Heat capacity ratio	k	1.403	1.0936	-
Specific gas constant	R_s	287	56.9	J/(kgK)

The temperature change in the arc compartment, in interval Δt, is calculated according to:

$$\Delta T_1 = \frac{\Delta Q_1 - \Delta m_{12}(C_p - C_v)\cdot T_1}{m_1 \cdot C_v}, \quad (1)$$

with following notations:

ΔQ_1 – the portion of electric energy used to heat the gas, including the exothermic reaction between the evaporated electrode material and gas,

C_p – specific heat capacity at constant pressure [$Jkg^{-1}K^{-1}$],

C_v – specific heat capacity at constant volume [$Jkg^{-1}K^{-1}$],

m_1 – mass of the gas [kg],

Δm_{12} – mass flow from the arc compartment into the exhaust compartment after the opening of the bursting disc [kg].

The portion of electric arc energy used to heat the gas in this model also considers the energy of exothermic/endothermic reaction between the gas and evaporated electrode material. It is calculated using the following equation:

$$\Delta Q_1 = k_p \cdot P_{el} \cdot \Delta t, \quad (2)$$

Where k_p is the heat transfer coefficient and P_{el} is the electrical arc power.

The temperature of gas T_1 in the arc compartment after time *t* is obtained by summing up all the changes of temperature ΔT_1. The gas pressure in arc compartment after time *t* is calculated from the equation of the ideal gas state:

D. Gorenc, K. Flegar, I. Lončar, E. Plavec, Simulation and Measurement of Pressure Rise in GIS 145 kV due to Internal Arcing, Journal of Energy, vol. 67 Number 3 (2018), Special Issue, p. 14–19

$$p_1 = \frac{(\kappa - 1)}{V_1} \cdot m_1 \cdot C_v \cdot T_1, \quad (3)$$

Where k is the heat capacity ratio and is the volume of the arc compartment.

After opening of bursting disc, the mass flow from the arc compartment, in interval , is calculated according to:

$$\Delta m_{12} = \alpha_{12} \cdot A_{12} \cdot \rho_{12} \cdot w_{12} \cdot \Delta t, \quad (4)$$

with following notations:

α_{12} – discharge coefficient (considering the contraction of gas flow through an opening),

A_{12} – bursting disc opening cross-section area [m²],

ρ_{12} – gas density within the opening [kg/m³],

w_{12} – gas velocity within the opening [m/s].

The total mass flow (kg) from the arc compartment after time *t* is calculated by summing up all the changes while the remaining gas mass in arc compartment is calculated by subtraction of the total mass flow from the initial mass. The temperature change in the exhaust compartment after opening of the bursting disc is calculated using the following equation:

$$\nabla \Lambda^{\Im} = \frac{\text{ww}^{\Im} \cdot \text{C}^{\text{h}}}{\nabla \text{ww}^{\text{I5}}(\text{C}^{\text{b}} \cdot \Lambda^{\text{I}} - \text{C}^{\text{h}} \cdot \Lambda^{\Im}) - \nabla \text{ww}^{\Im\Im} \cdot (\text{C}^{\text{b}} - \text{C}^{\text{h}}) \cdot \Lambda^{\Im}}, \quad (2)$$

Where is the gas mass and is the gas mass flow from the exhaust compartment into the environment.

The enhanced model with real gas/plasma properties, evaporation, ablation and exothermic reaction

The equations for temperature and pressure rise in the arc and exhaust compartment are derived with the assumption of ideal gas. The model is considering the real properties of gas/plasma which, in this case, consist of SF_6 gas and evaporated electrode material. For this purpose, tables with thermodynamic properties of gas/plasma for pure SF_6 and mixtures of SF_6 and evaporated copper at concentrations of 10%, 20%, 30%, 50% and 100% were prepared. The same was made for the mixture of SF_6 and evaporated aluminum. The influence of evaporated methane CH_4 on the thermodynamic properties of mixture is neglected due to low expected concentration. The temperature range in the tables is between 300 K and 10000 K, the pressure range is between 0.1 MPa and 10 MPa. The tables were prepared using the software named "Chemical Equilibrium with Applications" (CEA) [4]. For illustration, Fig. 2 shows C_p for the pure SF_6 gas and also for the mixture of SF_6 and evaporated Cu and Al, respectively. The curves are illustrated at pressure value of 1 MPa. The enhanced model is applicable for the temperatures up to 10000 K.

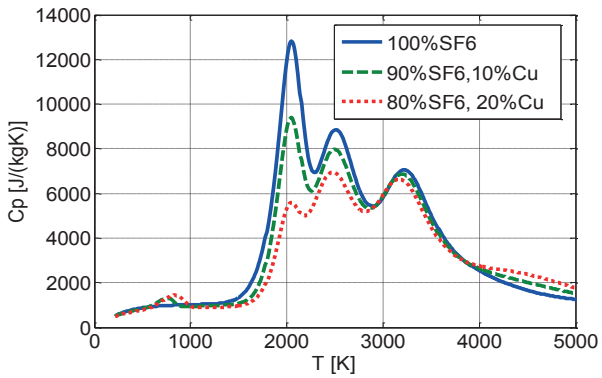

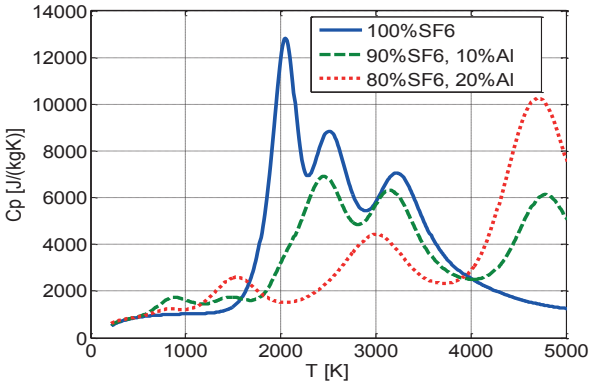

Fig. 2 C_p for pure SF_6 gas and mixture of SF_6 gas and evaporated Cu/Al at pressure of 1 MPa

The mass of evaporated electrode material, in interval , is calculated using the following equation:

$$\Delta m_{evap} = \frac{k_{evap} \cdot P_{el} \cdot \Delta t}{W_{evap}}, \quad (6)$$

Where k_{evap} is the evaporation factor which shows the portion of electric arc energy consumed on the electrode evaporation and is the specific energy required for evaporation of electrode material (Table II).

The mass of evaporated insulation material from the bushing plate in interval is calculated using equation:

$$\Delta m_{abl} = \frac{k_{abl} \cdot P_{el} \cdot \Delta t}{W_{abl}}, \quad (7)$$

Where W_{ex} is the ablation factor which shows the portion of electric arc energy consumed on the ablation of insulation material and is the specific energy required for ablation of insulation material.

Evaporation factor and ablation factor depend on material and they are determined experimentally i.e. by measuring the mass of evaporated material and electric arc energy, both of them are less than 1. The contribution of exothermic/endothermic reaction between the gas and the electrodes material on the temperature rise considers the additional energy source in arc compartment:

$$\Delta Q_{ex} = W_{ex} \cdot \Delta m_{evap}, \quad (8)$$

Where is the specific generated heat of exothermic/endothermic reaction [J/kg] (Table II).

If k_{evap} and are known and the contribution of exothermic/endothermic reaction is calculated according to (8), then the factor in this model cannot be greater than 1 as it was the case in the basic model with the constant gas properties. Namely, the sum of should be equal to 1 and it represents the law of conservation of energy, if the losses are neglected. The evaporated electrode material and the evaporated insulation material represent the heat source or heat sink when mixing with the gas. Therefore the temperature change in arc compartment is calculated according to:

$$\Delta T_1 = \frac{\Delta Q_1 + \Delta Q_{ex} - \Delta m_{12} \cdot (h_1 - u_1) + \Delta m_{evap} \cdot (u_{evap}(T_{evap}) - u_{evap}(T_1)) + \Delta m_{abl} \cdot (u_{abl}(T_{abl}) - u_{abl}(T_1))}{m_1 \cdot C_{v1}}, \quad (9)$$

with the following notations:

h_1 – specific enthalpy of gas/plasma in arc compartment [J/kg],

u_1 – specific internal energy of gas/plasma in arc compartment [J/kg],

u_{evap} – specific internal energy of the evaporated electrode material [J/kg],

T_{evap} – evaporation temperature of electrode material [K],

u_{abl} – specific internal energy of the evaporated insulation material [J/kg],

T_{abl} – ablation temperature of the insulation material [K].

Neglecting the chemical reactions between the gas from the arc compartment and the gas in exhaust compartment, the temperature change in exhaust compartment, in the interval , is calculated using the equation:

$$\Delta T_2 = \frac{\Delta m_{12} \cdot (h_1 - u_2) - \Delta m_{23} \cdot (h_2 - u_2)}{m_2 \cdot C_{v2}} \quad (10)$$

Where h_2 is the specific enthalpy of the gas in exhaust compartment [J/kg] and is the specific internal energy of the gas in exhaust compartment [J/kg].

INTERNAL ARC DEVELOPMENT TESTS

Test model

For the purpose of verifying the mathematical model, two configurations of the test model were designed and tested (Fig. 3). A total of 4 tests were performed. In the first two tests the arc has been initiated between the electrodes with the round cross-section (Fig. 4a) using the test configuration illustrated in Fig. 3a. In the first test the copper electrodes were used, while in the second they were replaced with the aluminum electrodes. Since the voltage source in the test laboratory was limited to about 600 V, the initial spacing between the electrodes, on which the arc was initiated, was only 3-4 mm. The initial SF_6 gas pressure in the test compartment was 0.6 MPa, while the pressure in the protective enclosure was 0.1 MPa. The volume of the test compartment is 0.3 m^3, while the volume of the protective enclosure is 2.4 m^3. The disc bursting pressure is 0.9 MPa ±5%, and the cross-section area is 0.009 m^2. During the test, arc voltage and current, the pressure in test compartment and protective enclosure, were measured. After the test, electrode material erosion was measured. The erosion of insulation material (in the tests no. 3 and 4) could not be accurately measured due to relatively large weight of the bushing plate compared to the amount of eroded insulation material, and also because of the fact that at the same time the erosion of cast copper electrodes in the bushing plate occurred. After the test, based on the measurements of the arc voltage and current, the electrical power and total arc energy were calculated.

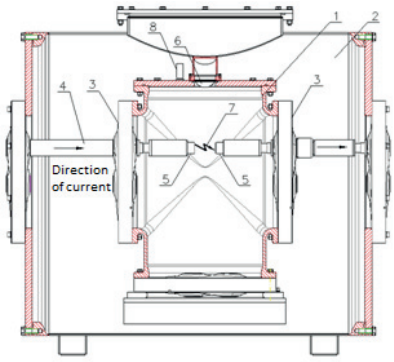

a)

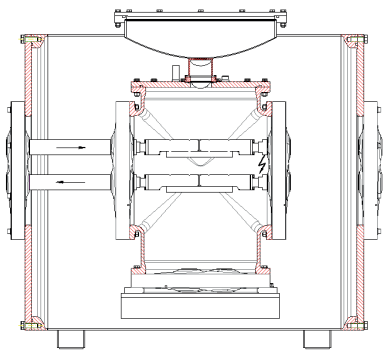

b)

Fig. 3 The cross-section of the test configurations for development testing on internal arc (1. test compartment, 2. protective enclosure, 3. bushing plate, 4. conductors, 5. changeable electrodes, 6. bursting disc, 7. electric arc, 8. pressure sensors)

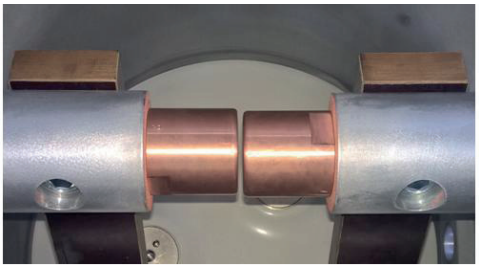

a)

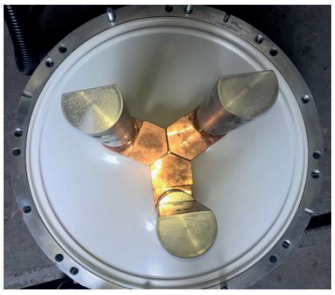

b)

Fig. 4 Electrodes for single-phase fault a) and three-phase fault b)

Fig. 5 Internal arc development testing in Končar – High Power Laboratory

Test results

The test results are shown in Table IV and figure 6.

Table IV Test results

Test no.	1	2	3	4
Test configuration	Figure 3a)	Figure 3b)		
Electrode material	Cu	Al	Cu	Al
Arc fault type	Single-phase	Three-phase		
Arc current [kA]	40	40	40	40
Arc duration [s]	0.36	0.114	0.42	0.37
Electric arc energy [MJ]	1.42	0.52	2.6	2.95
Max. pressure rise in test compartment [MPa]	0.35	0.32	0.4	0.85
Max. pressure rise in protective enclosure [MPa]	-	0.15	0.15	0.3
Bursting disc opening time [s]	0.65	0.6	0.38	0.18
Electrodes material erosion [g]	347.5	34.5	773.5	505.5

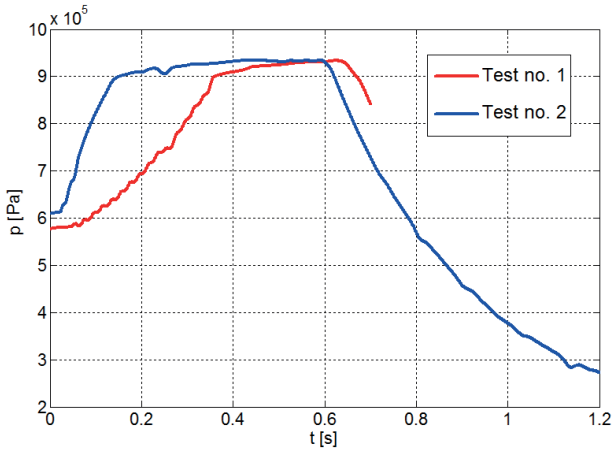

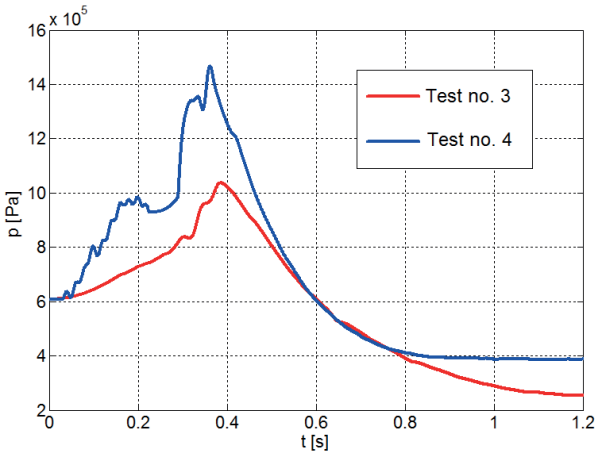

Fig. 6 Measured pressure in the test compartment

By analyzing the pressure curves in the tests no. 1 and 2, it can be seen that the maximum pressure rise is almost the same for copper and aluminum electrodes although the electric arc energy was 2.7 times smaller in the test with aluminum electrodes. The pressure gradient is also significantly higher in the test with aluminum electrodes. The bursting disc in both tests operated long after the arc was extinguished, which can be explained by the fact that for equalizing of the temperature, and thus the gas pressure, throughout the test compartment take some time.

In the tests no. 3 and 4, for approximately the same amount of electric arc energy, the double increase in pressure rise was obtained in test with aluminum electrodes. Although the bursting disc operated, the pressure continued to increase until the arc was extinguished. This is especially emphasized in the test no. 4 with aluminum electrodes.

The equalization of the pressure in the test compartment and protective enclosure after the arc is extinguished and the disc opened, will take less in the tests with higher maximum pressure (and higher maximum temperature) due to higher speed of sound at higher temperatures. Except in test no. 2, in all other tests, a significant erosion of the electrodes occurred. Erosion is partly a consequence of melting and partly of evaporation of electrode material. Due to the erosion of the electrodes, the distance between the electrodes increases, which increases the arc voltage. At the moment when the arc voltage value approaches to the maximum source voltage, the arc is extinguished. It should be noted that in the case of type test, due to greater distance between the electrodes, it is possible to expect up to ten times greater electric arc energy than it was achieved on the development test.

VERIFICATION OF THE MATHEMATICAL MODEL WITH THE TEST RESULTS

As it is shown in [3], verification of the mathematical model comes down to determination of the heat transfer factor and discharge coefficient for which a good correlation between the measured and calculated pressure P1 in the test compartment is obtained (Fig. 7). Unlike [3], where the basic model with constant gas properties was used to verify the results of the calculation, an improved model with real gas/plasma properties is used in this paper. By changing the factor in the calculation, the increase rate of pressure is adjusted, and by changing the discharge coefficient the downstream of pressure curve after the disc bursting. Since the erosion of electrodes is simultaneously the result of melting and evaporation of the material, it was not possible to determine the evaporation factors of electrode material or ablation factors of insulation material from the results of the tests. Therefore, in this case, the factor also includes the contribution of the exothermic/endothermic reaction to the pressure rise and the factors and are set to zero.

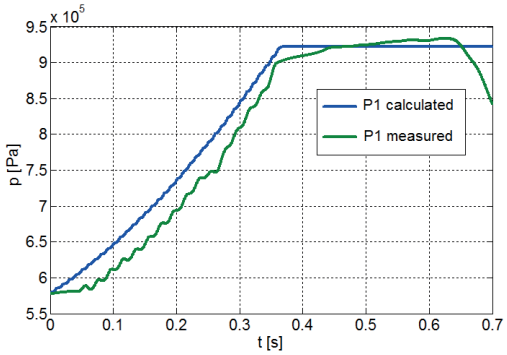

a) Test no. 1: k_p=0.9

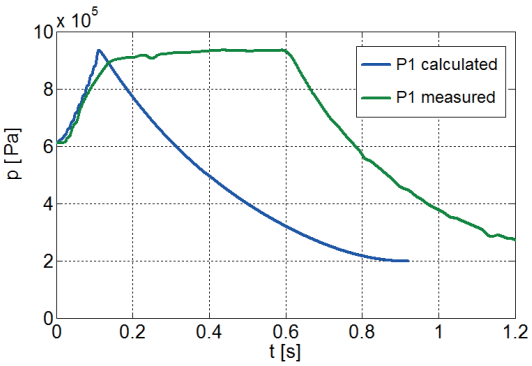

b) Test no. 2: k_p=2.35, α_{12}=0.7

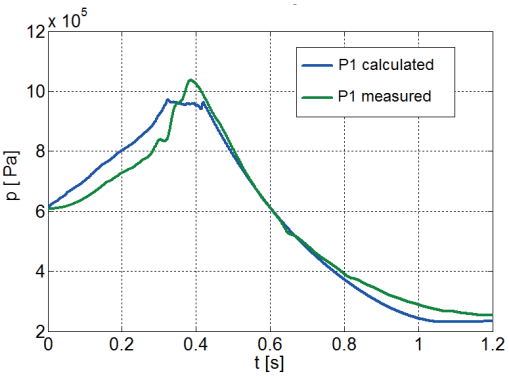

c) Test no. 3: k_p=0.9, α_{12}=0.7

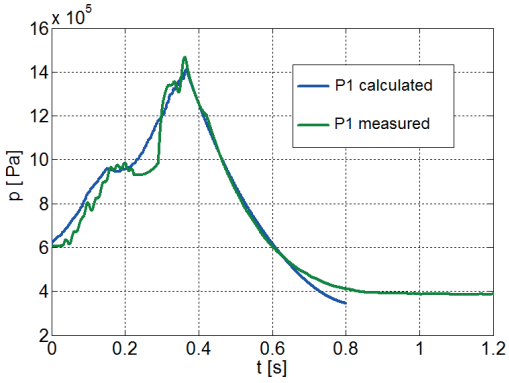

d) Test no. 4: k_p=2.3, α_{12}=0.7

Fig. 7 Verification of the mathematical model with the test results

D. Gorenc, K. Flegar, I. Lončar, E. Plavec, Simulation and Measurement of Pressure Rise in GIS 145 kV due to Internal Arcing, Journal of Energy, vol. 67 Number 3 (2018), Special Issue, p. 14–19

For the electric arc on the copper electrodes (tests no. 1 and 3), a very good correlation of the calculation results with the measurement results for the factor of 0.9 is achieved. On the other hand, for the electric arc on the aluminum electrodes (tests no. 2 and 4), the factors are 2.3 and 2.35 respectively. The discharge coefficient in test no. 1 was not possible to determine, since the downstream pressure curve, after the bursting disc operated, was not recorded to the end. In other tests, a good correlation of the calculation results with the measurement results was achieved for the discharge coefficient of 0.7.

CONCLUSION

In order to assess the GIS enclosure resistance on the internal arc at the upcoming type test, a program for the calculation of the pressure and temperature rise in the test compartment and protective enclosure due to an internal arc was developed. The basic model with constant gas properties shown in the A3.24 working group report was enhanced by the real gas/plasma properties, evaporation of electrodes material and ablation of insulation material. The contribution of the exothermic/endothermic reaction to the pressure and temperature rise was also taken into account. Unlike the basic model with constant gas properties applicable to the SF_6 gas temperature of 2000 K, the enhanced model is applicable to the temperature of 10000 K. The mathematical model is verified on the basis of the results of the GIS enclosure development test on internal arc. Satisfactory accuracy has been achieved in determining the maximum pressure and gradient of pressure rise in the test compartment and protective enclosure.

The tests performed on the copper and aluminum electrodes in SF_6 gas confirmed a significantly higher contribution of aluminum electrodes to the pressure and temperature rise in GIS enclosure (), compared to copper electrodes (). It can be concluded that for the same electric arc energy, in the case of aluminum electrodes, SF6 gas receives up to 2.5 times more heat than it is the case with the copper electrodes. Higher values of the factor in regards to the references can be explained by applying a mathematical model with the real gas properties. Namely, the increase of the gas temperature results in an increase in the specific heat capacity and the gas can absorb more heat with a lower temperature rise and pressure, respectively. In the model with the constant gas properties, which is mostly used in the references for the verification of calculation results with the measurement results, this effect is not considered.

For discharge coefficient the pressure drop curves have been calculated after the disc bursting and arc extinguishing and they are well matched with measured curves, indicating that gas flow through the opening and the pressure rise are well modeled.

However, the evaporation factor for electrode material could not be determined from the test results because the erosion of the electrodes is simultaneously the result of melting and evaporation of material. The ablation factor also was not possible to determine from the test results since it was not possible to precisely measure the erosion of insulation material from the bushing plate. Nevertheless, a computer program based on the presented mathematical model can be used to calculate the pressure and temperature rise in the test compartment and protective enclosure during the preparation of the test object for type test on internal arc.

BIBLIOGRAPHY

[1] IEC 62271-203:2011 „High-voltage switchgear and controlgear – Part 203: Gas insulated, metal enclosed switchgear for rated voltages above 52 kV“

[2] M. Binnendijk, G.C. Schoonenberg, A.J.W. Lammers, »The Prevention and Control of Internal Arcs in Medium-Voltage Switchgear“, CIRED 97, 2-5 June 1997, Conference Publication No. 438 IEE, 1997.

[3] N. Uzelac, M. Glinkowski, L. del Rio, M. Kriegel, J. Douchin, E. Dullni, S. Freitoza Costa, E. Fjeld, H-K. Kim, J. Lopez-Roldan, R. Pater, G. Pietsch, D. Reiher, G. Schoonenberg, S. Singh, R. Smeets, T. Uchii, L. Van der Sluis, P. Vinson, D. Yoshida „Tools for the Simulation of the Effects of the Internal Arc in Transmission and Distribution Switchgear“, Working Group A3.24 CIGRE, December 2014.

[4] https://www.grc.nasa.gov/WWW/EAWeb/ceaguiDownload-win.htm